# Quasiparticle calculation of the electronic band structure of the $(InAs)_1/(GaAs)_1$ superlattice

R. Padjen and D. Paquet*
*Centre Nationale d'Etudes des Telecommunications, Laboratoire de Bagneux, 196 avenue Henri Ravera, 92220 Bagneux, France*
(Received 2 April 1990; revised manuscript received 10 September 1990)

We present a screened-exchange calculation of the one-electron excitations of the strained pseudoalloy $(InAs)_1/(GaAs)_1$ grown on an InP substrate. The model adopted was the local-density-functional and quasiparticle self-energy approximation with a statically screened local dielectric matrix and the spin-orbit interaction term evaluated within degenerated perturbation theory. The gap calculated with the room-temperature lattice constant is 0.66 eV. The calculations of the GaAs and InAs bulk materials, both unstrained and strained on the InP substrate, were also performed and give somewhat underestimated values for the zone-center gaps and an excellent agreement with experimental results for the tetragonal and spin-orbit splittings. The dispersion curves and the contour plots of the valence density as well as of the density of the first conduction states are also displayed. The behavior of the dispersion curves very close to the zone center was analyzed both for the strained bulk materials and the $(InAs)_1/(GaAs)_1$ superalloy, leading to some interesting features.

## I. INTRODUCTION

The technique of molecular-beam epitaxy and its recent improvements like migration-enhanced epitaxy have recently spawned quite a few experimental studies[1-4] on the highly strained heterostructures like the InAs/GaAs short-period superlattices (SPS), which can be grown lattice matched on the InP substrate. Those superlattices are currently being studied for potential technological applications.[5] It is also interesting to compare the electronic properties of such tetragonal-symmetric ($D_{2d}$) materials to the cubic-symmetric ($T_{2d}$) alloys like $Ga_xIn_{1-x}As$. The features like the anisotropy of the electron effective mass and a lifting of the valence-band degeneracy have been observed in the strained SPS's.[6]

In this paper a model band-structure calculation of the $(GaAs)_1/(InAs)_1$ superlattice is investigated, taking explicitly into account the nonlocal screened exchange term in the crystal Hamiltonian. Due to the calculational complexity of the structure under study (the absence of the inversion center in the polar materials and a large dimension of the plane-wave basis due to a small Brillouin zone), we had to sacrifice some of the features of the most advanced first-principles calculations,[7,8] i.e., the nonlocality and the dynamics of the dielectric matrix. Those two features, though giving partially cancelling contributions to the one-electron spectra, influence to some extent the zone-center band gaps and are very important for the accurate determination of the local charge properties.

The rest of the paper is organized as follows. The technical details of the present approach are summarized in Sec. II. In Sec. III the results of the band-structure calculations for bulk GaAs and InAs materials, strained GaAs and InAs grown on InP substrates, and finally for the $(GaAs)_1/(InAs)_1$ superlattice on InP substrates are exposed and discussed. Section IV is reserved for a brief conclusion.

## II. DESCRIPTION OF THE MODEL

Any simple first-principles model for the semiconductor band-structure calculation suffers from poor predictions for the band gaps. They are much too small within the local-density approximation (LDA) of the density-functional method which, on the other hand, gives the most reliable valence-band wave functions. A fully self-consistent Hartree-Fock calculation on GaAs (Ref. 9) starting from an *ab initio* pseudopotential[10] and including explicitly the nonlocal exchange term has demonstrated the weakness of that approach when applied to the crystal-structure calculations. The zone-center gap of GaAs was computed to be 6.10 eV, as expected from a calculation lacking the exchange screening terms. A more serious drawback is much too low electron energies in the first conduction band at the zone edges. When the exchange term is schematically screened, e.g., by the Levine-Louie–model[11] dielectric matrix, the GaAs gap becomes indirect, indicating that the Hartree-Fock eigenfunctions are not a convenient basis set for any further perturbation-theory treatment of the crystal structure.

In a strict sense, in order to take fully into account the exchange screening one should compute the complete nonlocal and frequency-dependent dielectric matrix in the crystal using the random-phase approximation (RPA) based on the first estimate of the band structure and iterate until self-consistency is achieved. Such calculations are out of the scope of present methods, considering the formidable computational task of evaluating the dielectric matrix by the RPA in the crystal environment.

That program was partially implemented for the bulk semiconductors and for the Si/Ge superlattices in a recent series of papers.[7,8] In those calculations the LDA was used for the evaluation of the basis set of functions. Actually, the LDA basis is quite close to the self-consistency since the LDA Hamiltonian contains a local

 

screened-exchange term.

The starting point of the present approach is the LDA calculation of the Bloch functions to be used in the subsequent perturbation treatment of the screened-exchange term. The pseudopotential used in the LDA is the *ab initio* norm-conserving potential,[10] using the Ceperley-Adler exchange-correlation functional.[21] All calculations have been performed in a plane-wave basis with a kinetic-energy cutoff of 18 Ry. The self-energy correction $\delta\Sigma$ to the LDA eigenvalues due to the exchange term screened by a statical and local dielectric matrix can be written as

$$\delta\Sigma_{n\mathbf{k}}=\langle n\mathbf{k}|\delta\Sigma|n\mathbf{k}\rangle = \sum_{m,\mathbf{q}}\sum_{\mathbf{G}}|\langle n\mathbf{k}|e^{i(\mathbf{k}-\mathbf{q}+\mathbf{G})\cdot\mathbf{r}}|m\mathbf{q}\rangle|^2\delta W(\mathbf{k}-\mathbf{q}+\mathbf{G}) , \tag{1}$$

where $(m,\mathbf{q})$ stand for the occupied states, $(n,\mathbf{k})$ for the occupied and unoccupied states, $\mathbf{G}$ is a reciprocal-lattice vector, and $\delta W(\mathbf{Q}=\mathbf{k}-\mathbf{q}+\mathbf{G})$ is the partially screened Coulomb interaction. Following Gygi and Baldereschi[13] the exchange screening is split into two parts: $\epsilon_{\rm SC}^{-1}(Q,\omega=0)$ denoting the diagonal part of the inverse dielectric matrix of the semiconductor fitted from the RPA calculations[14] and $\epsilon_M^{-1}(Q,\omega=0)$ representing the inverse of the homogeneous-electron-gas static Lindhardt function, which should be subtracted because the long-range metallic part of the screening has already been taken into account in the exchange-correlation part of the LDA functional:

$$\delta W(Q)=4\frac{\pi}{\Omega Q^2}[\epsilon_{\rm SC}^{-1}(Q,\omega=0)-\epsilon_M^{-1}(Q,\omega=0)] \tag{2}$$

in inverse Bohr units. We use the following parametrizations of $\epsilon_{\rm SC}^{-1}$ and $\epsilon_M^{-1}$:

$$\epsilon_{\rm SC}^{-1}(Q)=\frac{Q^2+\alpha^2\epsilon_0}{Q^2+\alpha^2} \tag{3}$$

and

$$\epsilon_M^{-1}(Q)=\frac{Q^2+Q^4}{k_{\rm TF}^2+[1+(1-1/\epsilon_0)\alpha^2]Q^2+Q^4} . \tag{4}$$

In the present calculation the value of the dielectric constant at the zone center, $\epsilon_0$, has been set to 10.9 and the value of the fitting constant $\alpha$ to 0.86.

One of the salient features in the treatment of the screened-exchange term is the evaluation of the singular integral over the Brillouin zone. We used the special-points method[15] in order to reduce the number of $q$ points in the LDA part of the calculation. Here we sketch the method of integration.

The LDA Bloch functions are expanded into plane waves:

$$\psi_{m\mathbf{k}}(\mathbf{r})=\sum_{\mathbf{G}}a_m^{\mathbf{k}}(\mathbf{G})e^{i(\mathbf{k}+\mathbf{G})\cdot\mathbf{r}} . \tag{5}$$

We define the density matrix in reciprocal space as follows:

$$\rho(\mathbf{q};\mathbf{G}_1,\mathbf{G}_2)=\sum_{m\ \rm occ}a_m^{*\mathbf{q}}(\mathbf{G}_2)a_m^{\mathbf{q}}(\mathbf{G}_1) , \tag{6}$$

and the mean value of the density matrix in the Brillouin zone as

$$\rho_{\rm av}(\mathbf{G}_1,\mathbf{G}_2)=\sum_{m\ \rm occ}\sum_{i=1}^{N}w_i\rho(\mathbf{q}_i;\mathbf{G}_1,\mathbf{G}_2) , \tag{7}$$

where $\mathbf{q}_i$'s denote the Chadi points and the $w_i$'s the weights of the points. We approximate the integral of the screened-exchange term, Eq. (1), by a sum of products of $\rho_{\rm av}$ matrix elements times energy denominators integrated over the Brillouin zone:

$$\delta\Sigma(\mathbf{G}_1,\mathbf{G}_2)=\sum_{\mathbf{G}'}\rho_{\rm av}(\mathbf{G}_1+\mathbf{G}',\mathbf{G}_2+\mathbf{G}')I(\mathbf{G}') , \tag{8}$$

where

$$I(\mathbf{G}')=\int\delta W(\mathbf{k}-\mathbf{q}+\mathbf{G}')d\mathbf{q} \tag{9}$$

is computed for each reciprocal-lattice vector $\mathbf{G}'$ at $10^6$ points in the Brillouin zone; all calculations in the present study were performed using two Chadi points. The spirit of this approach is based on the fact that the use of a relatively small number of Chadi points gives a good approximation for the calculation of the mean density matrix; on the other hand, the numerical evaluation for the singular three-dimensional integral (9) requires $10^6$ $\mathbf{q}$ points in order to decrease the error to under 0.01%.

## III. RESULTS

We have tested first the model on the cubic bulk semiconductors GaAs and InAs. The calculation has been performed with the lattice constants experimentally obtained at 300 K, as displayed in Table I. In the case of GaAs we were able to compare our results to the ones previously obtained with the same model. Our calculated GaAs gap without spin-orbit correction is 1.15 eV, compared to 1.22 eV obtained by Gygi and Baldereschi,[16] who calculated with lattice constants extrapolated to 0 K and used a different technique of integration over the Brillouin zone.[17] Our calculated gap is too small compared to the experimental value of 1.42 eV. The model used does not take into account the nonlocal and dynamic properties of the dielectric matrix. The more elaborate models incorporating the nonlocal and dynamic screening render the results closer to the measured value: the fully converged calculation with a cutoff at 18 Ry by Zhang *et al.*[8] gives a gap of 1.29 eV; and Godby *et al.*[7] obtained 1.53 eV, but their cutoff is at 12 Ry. Both results include the spin-orbit corrections. The discrepancy

TABLE I. Experimentally found lattice constants (Ref. 17) expressed in atomic units and used in the present calculation for the cubic crystals.

| GaAs | InP | InAs |
|---|---|---|
| 10.681 | 11.094 | 11.949 |

TABLE II. The lattice constants in atomic units evaluated within the elasticity approximation (Ref. 18) and used in the present calculation in the case of tetragonal materials.

| | $a_{x,y}$ | $a_z$ |
|---|---|---|
| GaAs | 11.094 | 10.038 |
| InAs | 11.094 | 11.834 |
| GaAs/InAs | 11.094 | 11.071 |

between the gap calculated by Zhang *et al.* and the measured values leaves room for core corrections that are large for the state $\Gamma_{6c}$.

In the case of InAs the calculated LDA direct band gap is very small—just a few meV—but this feature does not interfere with the iteration process since the separation between the valence and the conduction states is larger than 1 eV at the Chadi points and the wave function still represent a workable basis for the quasiparticle calculations. The calculated quasiparticle gap is 0.29 eV compared to the measured value of 0.354 eV, which is in better agreement with experiment than in the case of GaAs.

Next, we calculate the bulk GaAs and InAs matched to the InP substrate. The symmetry of these crystals is tetragonal (with point group $D_{2d}$). The lattice parameters evaluated within the elasticity approximation are shown in Table II. The results are summarized in Tables III and IV. Note the very good agreement between the calculated and measured deformation potentials.

The top valence level at the center of the zone is a $\Gamma_{7v}$ (heavy-hole) state for GaAs and a $\Gamma_{6v}$ (light hole) for InAs. In GaAs, which is uniaxially compressed while strained on InP, our calculation produced an anticrossing in the direction $\Gamma-Z$ of the bands originating from $\Gamma_{7v}$ and $\Gamma_{6v}$ levels, which are tetragonally split from the $\Gamma_{8v}$ cubic-symmetry level. It occurs between the (0,0,0.06) and (0,0,0.07) points of the Brillouin zone.

At the center of the zone we get large and opposite-sign heavy-hole–light-hole tetragonal splitting $E_{\mathrm{HH}}-E_{\mathrm{LH}}=-0.376$ for GaAs and 0.149 for InAs. Furthermore, the GaAs gap is reduced by the strain down to 480 meV, whereas the InAs gap increases to 338 meV. Due to the strain-induced coupling between cubic light holes and spin-orbit (s.o.) split-off states the apparent s.o. splitting is large in the tetragonal bulk materials: $E_{\mathrm{s.o.}}=249$ meV for GaAs and 527 meV for InAs.

TABLE III. The calculated and measured deformation potentials expressed in eV. $a$ denotes the deformation potential of the direct gap. $b$ denotes the shear deformation potential for a strain of tetragonal symmetry. The numbers in the parentheses represent some measured experimental values (Ref. 17).

| | $a$ | $b$ |
|---|---|---|
| GaAs | −7.3(−6.7) | −1.6(−1.7) |
| InAs | −5.4(−6.0) | −2.0(−1.8) |

TABLE IV. Some of the most important quasiparticle energies expressed in eV and measured from the top valence state at the point Γ. The asterisk indicates that the energy shown represents also the spin-orbit splitting. In the case of the tetragonal materials that split levels are denoted by HH for the heavy hole and LH for the light hole. s.o. denotes the spin-orbit split-off level The numbers in parentheses represent the experimentally found values (Ref. 17).

| | $\Gamma_{7v}$ | $\Gamma_{6c}$ | $X_{6c}$ | $X_{6c}$-$X_{6v}$ |
|---|---|---|---|---|
| | | Cubic | | |
| GaAs | −0.33* | 1.04 | 2.37 | 4.73 |
| | (−0.34) | (1.42) | (2.03) | (5.02) |
| InAs | −0.38* | 0.29 | 2.53 | 4.50 |
| | (−0.38) | (0.35) | | |
| | | Tetragonal | | |
| GaAs | −0.38 HH | 0.48 | 1.72 | 4.47 |
| | −0.63 s.o. | | | |
| InAs | −0.15 LH | 0.34 | 2.46 | 4.28 |
| | −0.58 s.o. | | | |
| GaAs/InAs | −0.05 LH | 0.66 | 2.61 | 3.74 |
| | −0.39 s.o. | | | |

The third part of the present work consists of the calculation of the electronic structure of the $(\mathrm{GaAs})_1/(\mathrm{InAs})_1$ superlattice grown on the InP substrate.[1] The values of the superlattice parameters within the anisotropic linear continuum elasticity approximation are shown in Table II. The atomic positions have been evaluated under the assumption that each layer of the superlattice is strained in a way that its in-plane parameter is matched to the one of the InP substrate. The respective positions of the atoms Ga, As, In, and As in the tetragonal unit cell are (0,0,0), (0.25,0.25,0.2328), (0,0.5,0.5), and (0.25,0.75,0.7672). The point-group symmetry of the crystal is $D_{2d}$ and the wave functions were expanded up to a cutoff of 18 Ry, the same as used in the

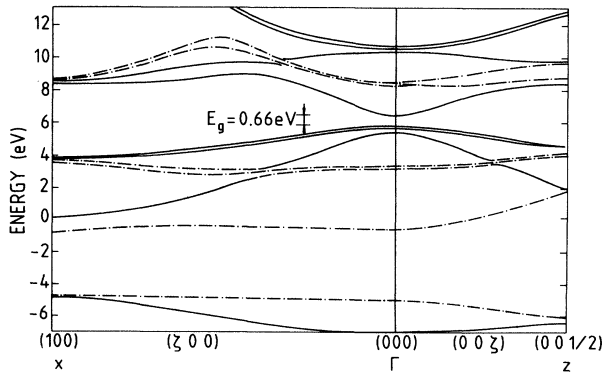


FIG. 1. Energy band structure for the $(\mathrm{GaAs})_1/(\mathrm{InAs})_1$ superlattice grown on an InP substrate in the [001] and [100] orientations. Sold line, states coming from an average tetragonal bulk material. Dash-dotted line, states coming from the folding due to the superperiodicity.

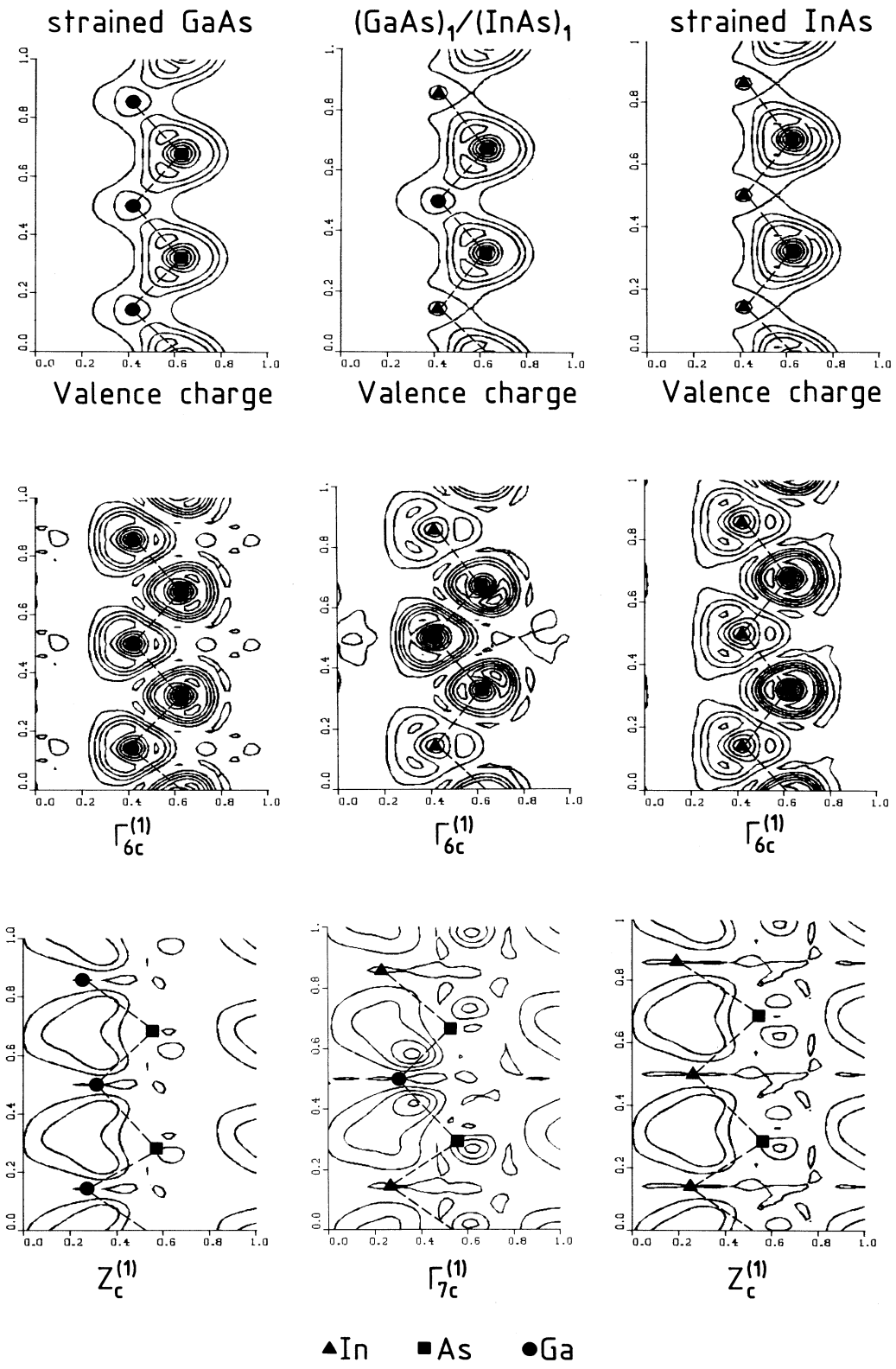


FIG. 2. Contour plot of the charge densities and of the first two conduction-state densities at the $\Gamma$ and $Z$ points of the Brillouin zone, in the plane closest to $(00\bar{1})$, and containing two successive bonds.

calculations for the bulk crystals. The main results are summarized in Table IV.

The calculated gap is 0.66 eV. The extrapolation of the existing measured gap values[2–4] to 300 K gives the results ranging from 0.72 to 0.80 eV, depending on the indium composition of the alloys. Having in mind the initial discrepancy between the calculated and the measured gaps of the constituent bulk semiconductors, our result for the superalloy seems quite reasonable.

The electron dispersion curves are drawn on Fig. 1, along the two directions $(\zeta,0,0)$ and $(0,0,\zeta)$. Although they seem somewhat intricate, we can get an initial understanding by splitting these curves into two classes. The solid lines stand for the dispersion curves that would have been obtained for an average bulk material around the Brillouin-zone center. The dash-dotted lines correspond to the folding due to the superperiodicity along the growth axis. Note the strong anticrossing between the spin-orbit valence band and the folding of the light- and heavy-hole bands. The second conduction state at the zone center (lying 1.92 eV above the first one) comes from the zone boundary of the first conduction state of an averaged bulk material. The tetragonal symmetry induces a rather slight splitting between the heavy and the light holes at the zone center ($E_{HH}-E_{LH}=50$ meV), a fact that is easily accountable when one realizes that the superlattice as a whole is nearly unstrained: its free equilibrium parameter nearly matches the InP substrate one.

Figure 2 shows the density contour plots computed in the plane $(01\bar{1})$ for strained GaAs, InAs, and for the superalloy in a plane very close to $(01\bar{1})$ and containing two successive Ga—As and As—In bonds.

## IV. SUMMARY AND CONCLUSION

In this paper we have presented a theoretical study of the electronic structure of the strained polar semiconductors based on the quasiparticle approach, with explicit evaluation of the Fock exchange operator. The same method was subsequently used for the calculation of the strained $(GaAs)_1/(InAs)_1$ superstructure. Our prediction of the deformation potentials is rather accurate. The direct band gaps obtained for GaAs, InAs, and consequently for the GaAs/InAs superlattice are too small, partially because the model employed does not take into account the nonlocal and dynamical properties of the Coulomb screening. On the other hand, the encouraging results for the deformation potentials should allow reliable estimates of the superlattice gaps from the measured gaps of the constituent materials. We hope that the simplified quasiparticle approach, together with the practical and accurate Brillouin-zone-integration technique adopted in this paper, will contribute towards numerical exploration of the small-period superlattices a step beyond the local-density approximation.

## ACKNOWLEDGMENTS

We gratefully acknowledge the generous allocation of Cray 2 computer time from the Centre de Calcul Vectoriel pour la Recherche. We are also indebted to Dr. J. Y. Marzin and Dr. J. M. Gérard, as well as to Professor R. Resta for stimulating discussions.

*Deceased.

[1]T. Fukui and H. Sato, Jpn. J. Appl. Phys. **23**, L521 (1984).

[2]M. Razeghi, P. Maurel, F. Omnes, and J. Nagle, Appl. Phys. Lett. **51**, 2218 (1987).

[3]B. T. McDermott, N. A. El-Masry, M. A. Tischler, and S. M. Bedair, Appl. Phys. Lett. **51**, 1830 (1987).

[4]J. M. Girard, J. Y. Marzin, B. Jusserand, F. Glas, and J. Primot, Appl. Phys. Lett. **54**, 30 (1989).

[5]J. Y. Marzin and J. M. Gérard, Superlattices Microstr. **5**, 51 (1989).

[6]J. M. Gérard *et al.*, Appl. Phys. Lett. **55**, 559 (1989).

[7]R. W. Godby, M. Schluter, and L. J. Sham, Phys. Rev. Lett. **56**, 2415 (1986); Phys. Rev. B **36**, 6497 (1987); **37**, 10 159 (1988).

[8]S. B. Zhang *et al.*, Phys. Rev. B **40**, 3162 (1989).

[9]R. Padjen, D. Paquet, and F. Bonnouvrier, Int. J. Quantum Chem. Symp. **21**, 45 (1987).

[10]G. B. Bachelet, D. R. Hamann, and M. Schluter, Phys. Rev. B **26**, 4199 (1982).

[11]Z. L. Levine and S. J. Louie, Phys. Rev. B **25**, 6310 (1982).

[12]D. Ceperley and B. Adler, Phys. Rev. Lett. **45**, 566 (1980); J. Perdew and A. Zunger, Phys. Rev. B **23**, 5048 (1981).

[13]F. Gygi and A. Baldereschi, Phys. Rev. Lett. **62**, 2160 (1989); F. Gygi, thesis, Ecole Polytechnique de Lausanne, 1988.

[14]A. Baldereschi and E. Tosatti, Phys. Rev. B **17**, 4710 (1978); R. Resta and A. Baldereschi, *ibid.* **23**, 6615 (1981).

[15]A. Baldereschi, Phys. Rev. B **7**, 5212 (1973); D. J. Chadi and M. L. Cohen, *ibid.* **8**, 5747 (1973).

[16]F. Gygi and A. Baldereschi, Phys. Rev. B **34**, 4405 (1986).

[17]Landolt-Börnstein, *Numerical Data and Functional Relationships in Science and Technology*, edited by O. Madelung and M. Schuls, New Series, Group III, Vol. 22, Pt. A (Springer-Verlag, Berlin, 1987).

[18]J. Y. Marzin, thèse d'état, Université de Paris VII, 1987.